


PAPER

[View Article Online](#)
[View Journal](#) | [View Issue](#)Cite this: *Sustainable Food Technol.*,
2025, 3, 1319Design and development of a parabolic trough
solar collector for pasteurization of milk†Shyam Kumar Singh *^{ab} and Ashis Kumar Datta^a

Milk, regardless of its end use, is required by law to be pasteurized to kill spoilage microorganisms and deactivate enzymes. Conventional methods of pasteurization use fossil fuels, which have a harmful effect on the environment. This study presents the design, optimization, fabrication, and experimental evaluation of a solar-powered milk pasteurization system using a parabolic trough collector (PTC) integrated with a single-axis solar tracking mechanism. The design parameters of the PTC including length (3 m), width (1 m), and rim angle (90°) were optimized using a combination of SolidWorks flow simulations and SolTrace, respectively. A single-axis solar tracking device was also developed to increase the efficiency of PTC, and this allowed the PTC to align with the direction of the Sun. The developed PTC was tested to determine whether it could achieve the temperature normally used for milk pasteurization. Milk and water temperature increased from an initial value of 33.03 ± 2.73 °C to 76.03 ± 1.35 °C, and 29.67 ± 2.86 °C to 80.85 ± 2.06 °C in 1 hour, respectively. Temperature increases of 12.43 ± 1.59 °C and 17.90 ± 2.42 °C were found for milk and water at a flow rate of 30 L h^{-1} in a single pass, respectively. This temperature increase suggests that the developed system has the potential to be used for the pasteurization of milk and similar liquid products utilizing solar energy.

Received 19th January 2025

Accepted 17th June 2025

DOI: 10.1039/d5fb00018a

rsc.li/susfoodtech

Sustainability spotlight

This study introduces a solar-powered parabolic trough collector (PTC) system designed for milk pasteurization, offering a renewable alternative to fossil fuel-based methods. Traditional pasteurization significantly contributes to greenhouse gas emissions, with substantial fossil fuel consumption. By harnessing solar energy, this work addresses the critical need for sustainable energy use in food processing, promoting cleaner technologies. Aligned with UN Sustainable Development Goals 7 (Affordable and Clean Energy), 12 (Responsible Consumption and Production), and 13 (Climate Action), this innovation contributes to reducing carbon footprints in food processing while supporting the transition to sustainable industrial practices.

1 Introduction

Milk and dairy products are consumed by billions of people worldwide. Beyond their nutritional significance, these products play a vital role in the livelihoods of farmers, processors, retailers, and other stakeholders, serving as an important source of income across the supply chain. Aside from its primary functions, milk from certain animals, especially cows and buffaloes, is consumed either as fresh milk or processed into various dairy products. Contaminated milk has been found to cause brucellosis, tuberculosis, scarlet fever, and Q fever.¹ Milk preservation practice by application of heat is believed to be as old as the domestication of the cow itself and the use of fire. The heating of milk before being fed to the infants was

suggested by William Dewes, almost 40 years before pasteurization came into existence after Pasteur's experiments.² The term pasteurization was coined in 1862 after Louis Pasteur discovered that most spoilage-causing bacteria, which were causing wine and beer to turn sour, were killed by the application of heat.³ Next, the method was used to increase the shelf life of milk. Therefore, pasteurization is defined as a process of heating and holding every particle of milk at a defined temperature for a sufficient amount of time to reduce pathogenic and spoilage microorganism counts to a predefined safe level.^{4,5} Originally, the temperature and time required for inactivation of *Mycobacterium tuberculosis* var. bovis, which was causing tuberculosis, were used to standardize the pasteurization process. But, presently, *Coxiella burnetii*, which causes Q fever, is used as an index microorganism to standardize the pasteurization process because it is one of the most heat resistant pathogens present in milk.^{2,3} Most commonly, two time-temperature combinations are used for pasteurization of milk: (i) low-temperature long time (LTLT), where milk is heated to 63 °C and held at that temperature for 30 minutes; (ii) high-temperature short time (HTST), where milk is heated to

^aDepartment of Agricultural and Food Engineering, Indian Institute of Technology Kharagpur, 721302, India^bDepartment of Food Science and Technology, University of California, Davis, 595 Hilgard Lane Davis, CA 956165, USA. E-mail: shksingh@ucdavis.edu† Electronic supplementary information (ESI) available. See DOI: <https://doi.org/10.1039/d5fb00018a>

72 °C and held for 15 seconds.¹ The time-temperature combination is not universal and varies depending upon the consistency of the product being pasteurized.

Pasteurization and other heat-based food preservation methods require a considerable amount of fossil fuel or electrical energy to achieve the necessary thermal conditions for microbial inactivation and product stability.^{5,6} Hall and Hedrick (1966) reported that approximately 20 kg of steam is required to process 100 litres of milk.⁷ Specifically, the HTST pasteurizer alone requires 7 kg of steam per 100 litres. A study done by Diakowska and Hall (1983) at the Food and Agriculture Organization found that thermal pasteurization consumes 684 MJ of thermal energy and 432 MJ of electrical energy per ton of milk per day.⁸ This indicates the amount of fossil fuel that would be required to generate such a tremendous amount of energy. The rising cost of fossil fuels and their negative impact on the environment have forced researchers and organizations throughout the world to focus on renewable sources of energy such as solar, nuclear, and wind energy. These fossil fuels release CO₂ and chlorofluorocarbons into the atmosphere, which are major contributors to global warming.⁹ Therefore, alternative sources of energy should be explored more to make the world a better place to live for future generations. Solar energy is abundantly available compared to other renewable sources of energy and has the potential to meet a sizeable fraction of the world's energy demand. Earth receives approximately 170 petawatts of solar energy, and it is estimated that 900 exajoules of energy can be generated from 84 minutes of solar radiation, and this energy can meet the energy demand of the whole world for one year (as of 2009).¹⁰ However, significant research and technological advancements are still required to optimize the efficient utilization of solar energy.

The concentrated solar power (CSP) approach has the potential to meet future energy demands. Among the widely used CSP technologies for energy generation are the parabolic dish, central receiver system, parabolic trough collector (PTC), and linear Fresnel reflector. Notably, the PTC has emerged as one of the most promising technologies, with increasing testing and implementation at the field level for power generation.^{10,11} PTCs are solar energy transformation systems that collect and focus sunlight from a large area onto a smaller receiver, enabling efficient thermal energy conversion.¹²

Several studies have explored the use of solar energy for various thermal applications, particularly in the agricultural and dairy sectors. Oparaku and Iloeje (1991) constructed a photovoltaic module to provide an independent, clean, and reliable electrical energy source for remote areas, recommending its use for water heating in micro-irrigation and dairy farms.¹³ Schnitzer, Brunner, and Gwehenberger (2007) reported that in the Australian dairy industry, 80% of the energy demand for processes requiring temperatures between 60 °C and 80 °C was met using solar energy.¹⁴ Franco *et al.* (2008) designed a Fresnel-type concentrator for pasteurizing goat milk as part of artisan cheese production, successfully pasteurizing 10 liters of milk per hour.¹⁵ Atia *et al.* (2010) used a 1.2 m² solar flat plate collector to pasteurize milk at temperatures of 63 °C and 72 °C.¹⁶ Additionally, da Silva *et al.* (2016) employed a flat-plate solar

collector to treat water at various temperatures and durations, confirming its microbiological safety by testing for total coliforms and *Escherichia coli*.¹⁷

Despite these advancements, to the best of our knowledge, no previous studies have examined the application of PTC systems specifically for milk pasteurization. Therefore, this study investigates the capability of the PTC as an efficient and promising device for milk pasteurization, expanding its potential applications beyond power generation into the food processing sector.

The dilute nature of solar energy is one of the main challenges associated with the use of parabolic trough collectors (PTCs), as it reduces the efficiency of any solar collector. To address this issue, a solar tracker can be used, which follows the position of the Sun throughout the day to ensure that the maximum amount of sunlight falls on the collector surface. Khan *et al.* (2010) developed a tracking system using an ATMEGA32 microcontroller and cadmium sulfide (CdS) photoresistors.¹⁸ Their system performed well under both normal daylight and adverse weather conditions. Studies have shown that adding a single-axis tracker can increase the energy output of a system by 12–20% compared to a stationary solar system.¹² The climatic conditions in India are highly suitable for harnessing solar energy, as the country receives approximately 250–300 sunny days per year, with solar radiation levels ranging from 4 to 7 kWh m⁻².¹⁹ Therefore, there is great potential for using solar energy for various applications in India.

In this study, a pasteurization unit was developed to utilize solar energy, and its effectiveness was evaluated to determine whether it could achieve the temperatures required for milk pasteurization. SolidWorks flow simulation and SolTrace were used to optimize the length, width, and rim angle of the PTC. Additionally, a single-axis solar tracker was developed using light-dependent resistors (LDRs) and voltage comparators.

2 Materials and methodology

2.1. Parabolic trough collector and its design parameters

PTCs (as shown in Fig. 1) represent the most promising technique for harnessing solar energy and are able to heat fluids to

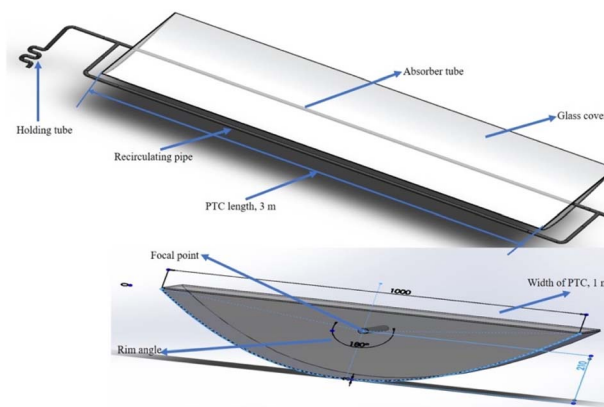


Fig. 1 Dimensional schematic of the parabolic trough collector (PTC) showing the major components, including the reflector, receiver tube, support structure, and alignment details.



a temperature of 310 °C.²⁰ A PTC consists of a reflector, receiver tube, tracking device, and reflector support structure. These heated fluids are used for industrial hot water, solar thermal electricity, or steam production.²¹ It comprises a reflector support structure in the shape of a parabola, on which a surface made of a reflecting material is mounted. It has a cylindrical receiver assembly placed at the focus of the parabola with the selective coating material to allow for maximum absorption of incident rays and is enclosed inside a glass envelope to reduce convective losses.²²

The property of a PTC, which makes it the most favourable device for solar energy conversions, is that all the rays which hit the reflecting surface get reflected at a single point, which is the focal line of the parabola, thus minimizing the losses. The design of the PTC includes optimization of the length of the parabola, rim angle, aperture width, receiver tube diameter, and focal length of the parabola in accordance with the desired end result.²³ Conventional techniques for designing equipment are based on trial and error, which is time-consuming and costly. Mathematical modelling and simulation tools can help in resolving these issues. It allows the study of how changing parameters, such as the rim angle and the width of the parabola, affect a PTC's ability to reflect and concentrate incident solar rays onto the receiver area.²⁴ Thus, modelling reduces the cost and labour requirements associated with conventional trial and error methods and also allows us to understand things at a deeper level.²⁵ Thus, SolTrace and SolidWorks flow simulation tools were used to optimize the rim angle, length, and width of the parabola.

2.2. Rim angle (ϕ_r) optimization

The rim angle (ϕ_r) refers to the angle measured from the edge of the collector to the line perpendicular to the collector's surface that intersects at the focal point.²⁶ SolTrace is optical modeling software developed by the National Renewable Energy Laboratory (NREL, USA), which was used for the optimization of the rim angle. The rim angle optimization with SolTrace was done in 4 stages following the procedure developed by Bharti and Paul (2017) with slight modifications.²⁶ In the first stage, the shape of the Sun was defined as a pillbox with a 4.65 milliradian half-angle from the centre. The second stage consists of assigning optical properties to the parabola surface and tube. The optical properties of the parabola material were a reflectivity of 0.9 and a transmissivity of 0.05, whereas the receiver tube properties used were a reflectivity of 0 and a transmissivity of 0, respectively. The tube was assumed to have the properties of a perfect black body. In the third stage, the geometry of the PTC was defined. In the final stage, a desired number of rays and direct normal irradiance were chosen (in this study 10^6 rays and 800 W m^{-2} irradiance were used), ray tracing was done, and the results were plotted. With a fixed length and width of the parabola, the rim angle was varied, and the effect of varying rim angles on the concentration of rays on the receiver tube was observed, and the rim angle which directed the maximum number of incident Sun rays on the receiver tube was selected.

2.3. Receiver diameter

The receiver tube in a parabolic trough collector must be appropriately sized to capture the concentrated solar radiation effectively. As the parabolic mirror focuses sunlight along its focal line, the reflected rays form a concentrated region of solar flux rather than a sharp point. Therefore, the diameter of the receiver tube should be sufficient to intercept this concentrated solar energy, ensuring minimal optical losses and maximizing thermal efficiency; a representation of this can be visualized in Fig. 4.²⁷ John and William (2006) gave the following theoretical equation to calculate the diameter of the cylindrical tube, which would intercept all the reflected beams.²⁸

$$D = \frac{a \sin 0.267}{\sin \phi} \quad (1)$$

This equation is valid for a surface free from any roughness and surface aberrations, and because of that, more spreading of the beam may occur. To account for this, a tube with a slightly larger diameter than what is calculated using the above equation should be used.

2.4. Optimization of the aperture width and length of the parabola

Optimization of the aperture width is essential because it will govern the amount of radiant energy falling on the reflector. Both very small and large aperture widths should be avoided. A small aperture, regardless of the rim angle, will receive a low amount of solar rays, whereas a large aperture increases the focal length and creates a darkening effect with large rim angles, which eventually reduces the efficiency of the PTC.²⁹ SolidWorks (Waltham, MA, USA) flow simulation was used for the optimization of the aperture width and length of the parabola, and an approach outlined by Bellos *et al.* (2018) were used with modification to suit the current study.²⁴ Initially the geometry was created, and thereafter suitable materials were selected for different parts of the PTC, and then the boundary conditions were chosen, and finally, the solar radiation information, which is most crucial for the success of a PTC, was assigned. Solar data were fed to the software using the inbuilt geographical option, which takes the data according to the location. Fluid properties used for simulation are given in Table 1. The trough is assumed to reflect almost all the incident rays on the focal line of the parabola; therefore, it was assigned the property of a symmetry object to account for the mirror-like properties of the trough. Glass cover transmittance was set to 0.95 for the analysis, and the absorptivity of the pipe was 0.95 to

Table 1 Milk and water properties used for simulation

Property	Milk	Water
Density (kg m^{-3})	1030	999.79
Dynamic viscosity (Pa s)	0.0012	0.00179
Specific heat ($\text{J kg}^{-1} \text{K}$)	3930	4219.9
Thermal conductivity ($\text{W m}^{-1} \text{K}$)	0.491	0.561



ensure that all the rays get absorbed to the pipe. The following assumptions were made for simulation:

- Steel was assigned to the receiver tube, and an absorptivity of 0.95 was assigned, so it acts as a black body.
- The cover was made transparent to solar radiation by giving it a transmittance of 0.95.
- Polished aluminium was selected for the parabolic trough so that almost all the incident rays get reflected to the receiver tube.
- To create a closed volume, lids were applied to both ends, and they were selected as insulators.

In the next stage, the boundary conditions were defined. The inlet mass flow rate and inlet temperature were assigned to the inlet lid, the flow was selected to be fully developed, and the pressure of the outlet was determined in each case. The simulation was conducted at six different flow rates: 30, 35, 40, 45, 50, and 55 L h⁻¹. These flow rates were selected based on a preliminary study. Next, radiation surfaces were defined to ensure that proper reflection and transmittance were taking place. For all incoming rays to get reflected, the reflector surface was set as a symmetry boundary. After that, the mesh was generated, and the model was computed. SolidWorks flow simulation uses the Discrete Transfer Radiation Model (DTRM) for ray tracing. With varying widths and lengths of the parabola, various simulations were conducted and the inlet and outlet fluid temperatures were noted, and the configuration which gave a 20–25 °C increase in temperature during a single pass was selected, and the PTC was fabricated using those dimensions.

After optimization of the rim angle, width and length of the parabola, other parameters were calculated using the following equations (Valencia *et al.* 2014):³⁰

- (1) The focal length (f) is given as

$$f = \frac{W_a}{4 \left(\frac{\Phi_r}{2} \right)} \quad (2)$$

- (2) The radius (r_r) of the parabola can be calculated using

$$r_r = \frac{2f}{1 + \cos \Phi_r} \quad (3)$$

- (3) The vertical height (H_p) of the parabola can be calculated using

$$H_p = \frac{W_a^2}{16f} \quad (4)$$

- (4) Geometric concentration ratio (CR):

It is defined as the ratio of the collector aperture area to the receiver aperture area.

$$CR = \frac{A_c}{A_r} \quad (5)$$

where

W_a = aperture width; A_c = collector area; A_r = receiver area;
 f = focal length; ϕ_r = rim angle.

Table 2 Specifications of different parameters of the PTC

Parameters	Values
Focal length of the parabolic collector	0.209 m
Aperture width	1 m
The outer diameter of the absorber tube	0.0254 m
The inner diameter of the absorber tube	0.022 m
Length of the absorber tube	3 m
Concentration ratio (based on the projected area)	39.37
Rim angle	90°

2.5. Fabrication of different parts of the PTC

The fabrication was carried out under the guidance of workshop technicians at the Agricultural and Food Engineering Department, Indian Institute of Technology Kharagpur. The parameters of the parabolic collector as presented in Table 2 were used for the fabrication of the PTC.

The frame of the collector was fabricated using 4 mm thick and 20 mm wide steel strips. The frame was made as a parabolic trough-like structure for supporting the collector with a provision for holding the receiver tube using clamps. For a material to be used as a collector in a PTC, it should have very high reflectivity. For this study, a polished aluminium sheet was used, which has a reflectivity of up to 0.95. An aluminium sheet of an average thickness of 0.42 mm was used as a collector, which was fixed and riveted on the frame. The receiver in a parabolic trough collector serves a dual purpose: it collects concentrated solar radiation reflected by the parabolic mirrors and converts this energy into heat. This thermal energy is then transferred to a heat transfer fluid circulating within the receiver tube, which can be utilized for various applications such as power generation or industrial processes.³¹ For a receiver tube to do that, it should have a very high absorptivity in the visible range and low emissivity in the infrared range of the electromagnetic spectrum.²⁷ In this study, a black painted stainless steel cylindrical tube with high absorption was selected. The receiver tube of stainless steel (AISI 316) was clamped with the frame in such a way that the focal axis of the

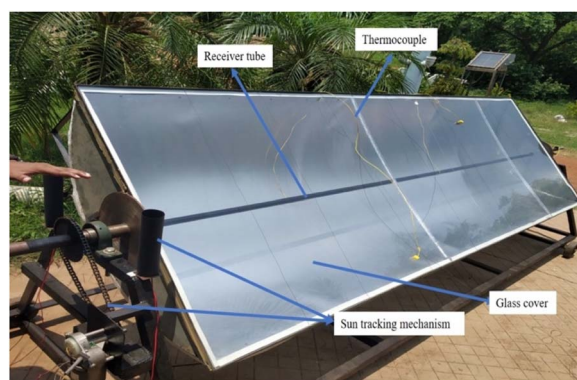


Fig. 2 Photograph of the fabricated parabolic trough collector system, highlighting key parts such as the aluminium reflector, black-painted stainless steel receiver tube, tracking apparatus and glass enclosure.



collector passed through it. The receiver tube had flow regulating valves fixed at the inlet side. A glass sheath was placed around the receiver tube to reduce the conductive and convective losses, which prevented the air from flowing across the tube. In addition, the glass surface was evacuated and blocked by window glazing putty around the edges to reduce the conductive and convective losses further. The transmittance of the polycarbonate sheet used was around 0.85. A polystyrene (Thermocol) sheet of 1-inch thickness was used as an insulator on the device. It was stuck to the underside part of the parabolic trough using thin galvanized iron wires, which stretched across the polystyrene sheet, holding them very tightly. It was applied to avoid any loss of heat from the bottom part of the system. The fabricated system is shown in Fig. 2.

2.6. Development of a single axis solar tracking system

A single axis tracking system was developed. It was made using two LDRs whose resistance was inversely proportional to the amount of incident light¹⁸ and a voltage comparator (LM358 Dual Op-Amp), which served as the heart of the system, along with other components used (see Fig. 3). The circuit diagram was made using Proteus 8 Professional (Labcenter Electronics Ltd, Yorkshire, England). This tracking system would allow the PTC to be oriented towards the Sun throughout the day to get maximum utilization of incident rays. Resistors (R3 and R4) were connected in series with one of the LDRs. As the amount of incident rays' increases, its resistance decreases, and the voltage across the corresponding resistor increases. Similarly, R1 and R2 resistors were connected in series with the other LDR. When there was an appreciable difference in voltage output, the motor moved the system in either direction unless output from each LDR became equal. To allow the motor to be rotated in both clockwise and anticlockwise directions, an H-bridge (more on this can be found elsewhere³²) was formed using complementary symmetry transistors BC547 and BC557. N-Channel Power Metal Oxide Silicon Field Effect Transistors (MOSFETs) IRF540 and IRF9540 were used as switches in the circuit to form the H-bridge.

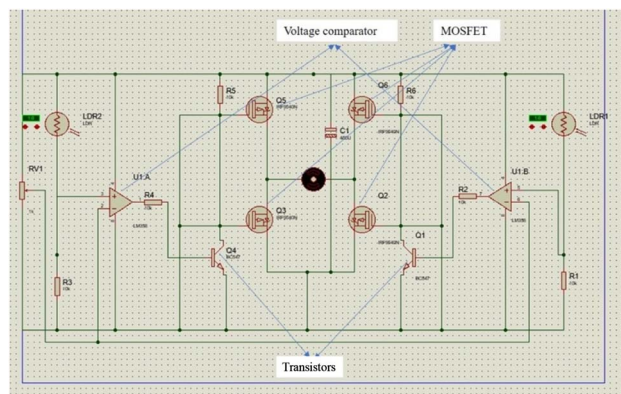


Fig. 3 Circuit diagram of the developed single-axis solar tracking system, illustrating the configuration of light-dependent resistors (LDRs), voltage comparator (LM358), H-bridge motor driver, and associated electronic components.

2.7. Testing of the developed pasteurization system

The equipment was tested on a flat surface using both water and milk. The collector surface was aligned along the north-south direction. Experiments were carried out between 10 AM and 2 PM to capture the maximum amount of solar energy. The milk used in the experiments was purchased from a local store located on the Indian Institute of Technology, Kharagpur campus. Two experimental setups were tested: in the first, the fluid was recirculated (the fluid exiting the first pass was sent back through the system, using the principle of regeneration), and in the second, the fluid was preheated to 60 °C using a water bath, with the flow rate adjusted using a piston pump. The flow rate was measured by collecting the liquid in a 1000 mL graduated measuring cylinder over one minute, timed with a stopwatch. Flow rates were varied at 30, 35, 40, 45, 50, and 55 L h⁻¹. The inlet and outlet temperatures were recorded using a K-type thermocouple (K-type, Model: Lutron TM-903 A). All experiments were conducted in triplicate.

3 Results and discussion

The rim angle governs the concentration of incident rays falling on the receiver, because as the rim angle changes focus changes, and this changes the shape of the parabola (as shown in Fig. 4). Therefore, optimization of the rim angle is crucial to ensure maximum utilization of incident solar energy. The results obtained with the optimization of the rim angle are shown in Fig. 4. It can be seen from Fig. 4 that with the increase of the rim angle, the focal length decreases, and as a result, a smaller number of reflected rays are concentrating on the receiver tube. Furthermore, with small rim angles, most of the rays are concentrated on the lower part of the receiver tube. On the other hand, with a very large rim angle, the reflected rays must travel a large distance, and, as can be seen from the figure as the rim angle goes beyond 90° the number of reflected beams on the receiver surface decreases. Thus, both very small and large rim angles reduce the concentration ratio and hence give a low energy output. After analysing the number of rays hitting

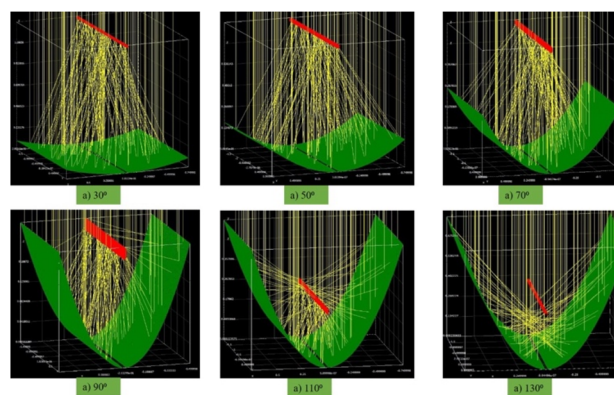


Fig. 4 Simulated effect of varying rim angles on parabola curvature and their impact on the concentration of reflected solar rays onto the receiver tube, based on optical modeling using SolTrace.





Fig. 5 Sequential images showing the position and movement of the PTC system throughout the day under the control of the developed solar tracker, capturing east-to-west sun tracking between 10:00 AM and 2:30 PM.

the receiver tube for each rim angle used, it was found that a PTC with a 90° rim angle was able to concentrate the maximum number of rays on the receiver tube, and hence it was selected for the fabrication of the PTC. A rim angle close to 90° has been commonly used in the design of most parabolic trough collectors (PTCs) reported in the literature.^{20,26,33–35}

Fig. 5 demonstrates whether the developed Sun tracking system is working efficiently or not. As can be seen from Fig. 5, the orientation of the PTC goes from facing east at 10:00 AM to almost straight at 12:30 PM and finally tilts towards the west at 2:30 PM. This shows that the developed tracking system is able to track the movement of the Sun effectively. A video has been provided as a supplement showing the working of the solar tracker. It was not possible to record a video for the whole duration of the experiment; therefore, the working of the tracking mechanism has been presented in the video. As shown in the video, when a hand is placed over one of the photoresistors, the parabolic trough collector (PTC) begins to move; once the hand is removed, the motion stops. This behaviour

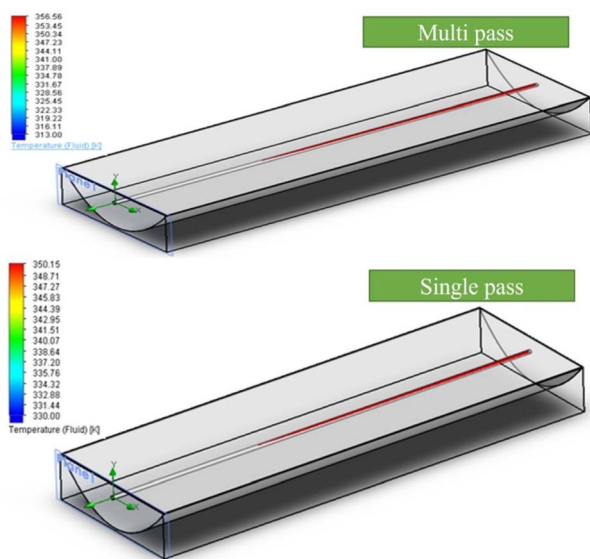


Fig. 6 Simulation results for milk heating at a flow rate of 30 L h⁻¹ using the optimized PTC configuration, showing predicted inlet and outlet temperatures under both multi-pass and single-pass operation.

indicates that covering the photoresistor creates a voltage difference between the sensors, which triggers the motor to activate. This observation further confirms the effectiveness of the developed tracking system in accurately following the Sun's position throughout the day.

To determine the best length and width for the system, simulations were performed across all tested flow rates as described in the Materials and methodology section; however, only the optimized results are presented here. As shown in Fig. 6, a PTC with a length of 3 m and a width of 1 m successfully achieved the necessary temperature rise (20–25 °C) under single-pass operation. In the multi-pass setup, simulations predicted that milk temperature would increase from 39.85 °C to 83.41 °C in one hour, surpassing the 72 °C threshold required for pasteurization. Similarly, in single-pass mode, the simulated milk temperature increased from 56.85 °C to 77 °C, resulting in a 20.15 °C rise. Based on these outcomes, the final design parameters for fabricating the PTC were selected.

After fabrication, the main goal was to experimentally verify the PTC's ability for applications like milk pasteurization. Experiments were carried out using both water and milk under two operating modes: multi-pass recirculation and single-pass operation with preheated fluid. Fig. 7 and 8 show the experimental results for water and milk in both configurations. Experiments were run at different flow rates for both liquids. In the multi-pass setup (where the fluid from the first pass was again allowed to pass to the inlet, and this process continued for 1 h, with temperature at the outlet of the pipe recorded after every 10 minutes), milk temperature rose from an initial 33.03 ± 2.73 °C to 76.03 ± 1.35 °C at 60 minutes (Fig. 7). Under similar conditions, water's temperature rose from 29.67 ± 2.86 °C to 80.85 ± 2.06 °C within the same period. These temperature increases exceeded the standard Low-Temperature Long-Time (LTLT, 63 °C) and High-Temperature Short-Time (HTST, 72 °C) pasteurization temperatures.

For the single-pass trials, fluids were preheated to 60 °C before entering the receiver tube, and the results are presented in Fig. 8. The maximum temperature increase for milk in

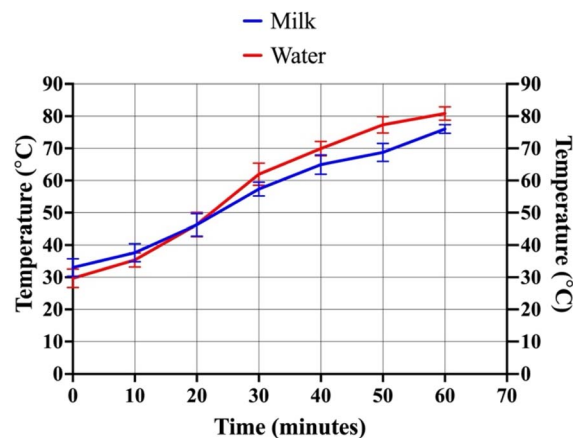


Fig. 7 Experimental results showing the increase in temperature for milk and water over 60 minutes during multi-pass heating using the fabricated PTC system demonstrating performance over 60 minutes.



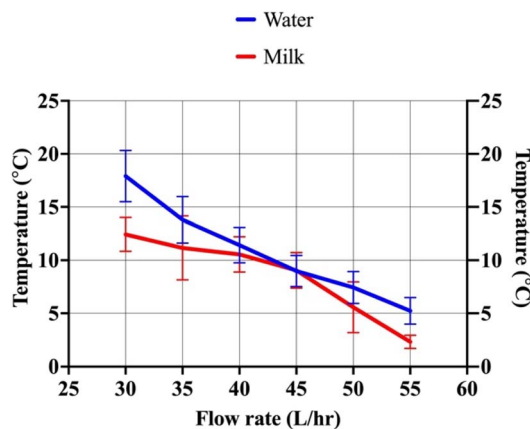


Fig. 8 Experimental results showing temperature increase for milk and water during single-pass heating trials at varying flow rates (30–55 L h⁻¹) using the fabricated PTC system, highlighting the effect of flow rate on thermal performance.

a single pass was 12.43 ± 1.59 °C (from 60 °C), reaching a final temperature of 72.43 °C at an optimized flow rate of 30 L h⁻¹. Similarly, water showed a greater temperature increase of 17.90 ± 2.42 °C (from 60 °C), reaching 77.90 °C, also at 30 L h⁻¹. The experimental results consistently demonstrated that the highest temperature increases for both fluids were achieved at the lowest tested flow rate (30 L h⁻¹), matching the simulation predictions. As the flow rate increased (e.g., to 35, 40, 45, 50, and 55 L h⁻¹), the temperature rise proportionally decreased. This inverse relationship occurs because a faster flow reduces the liquid's residence time inside the pipe, leaving less time to absorb the concentrated solar energy. This highlights a key operational trade-off between maximizing throughput and ensuring sufficient heating for pasteurization. Based on this, the optimal flow rate was determined to be 30 L h⁻¹, which produced temperature increases adequate for milk pasteurization and similar liquid products. With a properly designed holding tube, this system could be applied for commercial milk pasteurization.

Throughout the experimental trials, water consistently achieved a higher temperature rise compared to milk under identical operating conditions. This observed difference is directly attributable to the distinct thermophysical properties: milk contains a significant concentration of soluble solids (proteins, lactose, minerals, and fat), absent in pure water, which increase its specific heat capacity and density relative to pure water (as detailed in Table 1). Consequently, more energy is required to elevate milk's temperature by the same increment compared to water.

While the simulations provided a strong foundation, experimental validation revealed that the simulation model consistently but slightly overpredicted the outlet temperatures for both milk and water in both single-pass and multi-pass modes. However, the overall trend in the experimental results closely matched the model predictions. Such discrepancies are common in validating solar thermal system models and arise from several factors. A key issue was the inability to source

materials with properties exactly matching those assumed in the simulations. Material characteristics such as mirror reflectivity, glass transmissivity, and tube absorptivity significantly affect a PTC's optical and thermal performance, and even small differences can lead to noticeable performance gaps. For example, the thermal conductivity of the receiver tube, as well as specific surface treatments or geometries (like U-shaped, corrugated, or finned tubes), can enhance heat transfer in ways not fully captured by simplified models.³⁵

Another significant element contributing to the observed overprediction was the disparity in solar irradiation data utilized. The simulation model employed a constant solar irradiation value. In reality, solar intensity fluctuates throughout the day due to dynamic atmospheric conditions such as cloud cover and dust. Simulation models often rely on steady-state assumptions or simplified solar profiles, which inherently fail to fully capture the transient and variable nature of actual solar irradiance.^{36,37} The literature supports that such discrepancies between simulation and experimental results are typical in solar thermal system validation. Experimental validation studies for PTCs frequently report deviations, ranging from a few percentage points (e.g., 1.42–3.32% for thermal efficiency under clear/cloudy skies) to larger figures (e.g., 9.05% for thermal output).^{37,38} These studies consistently emphasize that accurately accounting for all sources of uncertainty and error, particularly those stemming from field measurements and material imperfections, is paramount for enhancing model accuracy.³⁷ Additionally, heat losses from components not fully integrated into the model, such as receiver support brackets, can also contribute to these observed discrepancies. The observed discrepancies between simulation and experimental results, particularly the overprediction, are a direct consequence of the inherent gap between idealized computational models and the complex realities of physical systems.

While other solar thermal systems have been explored for pasteurization, the PTC offers a distinct combination of advantages and limitations when compared to these alternatives. Flat-plate collectors (FPCs) are widely used for domestic hot water and low-temperature applications (30–90 °C). For example, Atia *et al.* (2011) used a 1.2 m² FPC to reach 63–72 °C within 3–19 minutes depending on solar intensity,¹⁶ while Obuoro *et al.* (2011) demonstrated a low-cost FPC system that pasteurized 40 L of milk in about 1.3 hours.¹³ Although FPCs can deliver hot water at temperatures up to around 100 °C and are simpler and less costly per unit area, they lose efficiency at higher temperatures due to greater heat loss. By contrast, the PTC's concentrating ability helps it maintain high thermal efficiency at elevated temperatures, making it better suited for continuous or larger-volume pasteurization where higher temperatures are needed. Evacuated tube collectors (ETCs) can achieve higher temperatures (50–200 °C) and work effectively even in low sunlight. Dobrowsky *et al.* (2015) used an ETC system to pasteurize approximately 500 L of milk, achieving bacterial inactivation at 72 °C, while other ETC systems provide hot water near 80 °C.³⁹ Although ETCs perform well, especially under colder or diffuse conditions, their lower concentration ratios can limit their ability to reach peak temperatures or



deliver direct heating as efficiently as PTCs. In this study, the developed PTC achieved comparable pasteurization temperatures, indicating similar effectiveness.

Fresnel concentrators and photovoltaic (PV)-based systems represent other alternatives but come with different trade-offs. Fresnel systems, such as the Arun system used in India, can handle large-scale pasteurization (20 000–30 000 L per day) but involve complex designs suited for industrial use.⁴⁰ On the other hand, PV systems convert sunlight into electricity, which is then used to power heating or advanced non-thermal methods like pulsed electric fields. While PV systems offer flexibility, they face energy conversion losses and long energy payback times compared to direct thermal systems like PTCs. Overall, the comparative analysis suggests that while various solar technologies can support milk pasteurization, PTCs offer a key advantage in directly and efficiently converting solar energy to medium-range temperatures (70–80 °C) without intermediate conversions. While flat-plate collectors are simpler but less efficient at these temperatures, and ETCs offer good performance under low sunlight but with lower concentration, PTCs provide robust and efficient heating, making them a promising and cost-effective option for decentralized milk pasteurization, particularly in regions with high direct solar radiation.

Though no quality tests were conducted in this study, as the sole goal was to determine if the developed system could achieve the required pasteurization temperatures, it is well known that any type of thermal treatment leads to changes in product quality.^{5,6} Solar thermal pasteurization, like conventional heat-based methods, can cause protein denaturation, slight nutrient losses, and minor alterations in sensory properties. However, since the primary driver of these changes is the temperature-time profile, not the heat source, milk processed with solar systems when properly controlled can achieve microbial safety and quality comparable to conventional pasteurization.

While the primary focus of this study was on the design, optimization, and technical evaluation of the PTC system for milk pasteurization, we acknowledge the importance of assessing its economic feasibility and energy efficiency compared to conventional systems. Conventional HTST pasteurization systems typically consume around 684 MJ of thermal energy and 432 MJ of electrical energy per ton of milk per day, requiring significant fossil fuel or grid electricity inputs.⁸ In contrast, the developed PTC system utilizes only freely available solar energy to achieve comparable pasteurization temperatures, suggesting substantial operational cost savings by eliminating fuel costs.

Although we did not conduct a detailed cost-benefit analysis in this study, the lower operating expenses, minimal maintenance requirements, and scalability of decentralized solar systems position PTC-based pasteurization as a promising alternative, especially in sun-rich regions where energy access or fuel costs are barriers. To fully validate the sustainability and scalability claims, future research needs to incorporate a detailed techno-economic assessment, including capital investment analysis, payback period estimation, life cycle

carbon footprint evaluation, and energy efficiency benchmarking against conventional pasteurization systems.

4 Conclusions

The increasing cost of electricity and fossil fuels, along with the adverse environmental effects associated with them, has forced researchers and lawmakers to focus more on renewable energy sources. This study successfully demonstrated the design, optimization, fabrication, and experimental validation of a parabolic trough collector system integrated with a single-axis solar tracker for milk pasteurization. Using simulation tools like SolTrace and SolidWorks, key design parameters including rim angle, aperture width, and parabola length were systematically optimized, resulting in a PTC configuration that maximized solar energy capture and efficient heat transfer. Experimental trials using both water and milk under multi-pass and single-pass conditions confirmed the system's ability to consistently achieve pasteurization temperatures, with optimal performance observed at a flow rate of 30 L h⁻¹. The solar tracker effectively maintained alignment with the Sun, enhancing the thermal performance of the system throughout the day. In summary, this work demonstrates the feasibility and potential of using concentrated solar power technologies, specifically PTC systems, for food processing in regions with abundant direct solar radiation. To advance the system toward commercial deployment, future studies should focus on the microbial inactivation, product quality, and detailed techno-economic and energy efficiency analyses to assess its long-term sustainability, cost-effectiveness, and scalability compared to conventional fossil fuel-based pasteurization methods.

Data availability

The raw data supporting the conclusions of this article will be made available by the authors on request.

Author contributions

Shyam Kumar Singh: conceptualization, methodology, experimentation, data analysis, and writing – original draft. Ashish Kumar Datta: advising, conceptualization, funding acquisition, reviewing, and editing.

Conflicts of interest

The authors declare no conflict of interest.

Acknowledgements

The authors would like to thank Mr Uttam Majumdar, G. Laxman Rao, Sudhip Khatua, and Tapas Midya, supporting staff at Agricultural and Food Engineering, Indian Institute of Technology Kharagpur, who helped in fabricating the system and in conducting the experiments.



References

- 1 P. W. Smith, *Milk Pasteurization Fact Sheet Number 57*, US Department of Agriculture Research Service, Washington, DC, 1981.
- 2 V. H. Holsinger, K. T. Rajkowski and J. R. Stabel, Milk pasteurisation and safety: a brief history and update, *Bull. - Off. Int. Epizoot.*, 1997, **16**(2), 441–466, DOI: [10.20506/rst.16.2.1037](#).
- 3 L. Meunier-Goddik, and S. Sandra, *Liquid Milk Products| Liquid Milk Products: Pasteurized Milk*. Encyclopedia of Dairy Sciences, 2nd edn, 2011, pp. 274–280, DOI: [10.1016/B978-0-12-374407-4.00280-6](#).
- 4 M. N. Ramesh, Pasteurization and food preservation, in *Handbook of Food Preservation*, CRC Press, Florida, 2020, pp. 599–608, DOI: [10.1201/9780429091483](#).
- 5 S. K. Singh, M. Ali, J. H. Mok and S. Sastry, Effects of field strength and frequency on inactivation of *Clostridium sporogenes* PA3679 spores during ohmic heating, *J. Food Eng.*, 2024, **375**(8), 112080, DOI: [10.1016/j.jfoodeng.2024.112080](#).
- 6 S. K. Singh, Ö. F. Çokgezme, M. M. Ali, A. E. Yousef, V. M. Balasubramaniam and S. Sastry, Ohmic heating inactivation of *Alicyclobacillus acidoterrestris* spores in apple and cranberry juice, *Innovative Food Sci. Emerging Technol.*, 2025, **102**(6), 104010, DOI: [10.1016/j.ifset.2025.104010](#).
- 7 C. W. Hall, and T. I. Hedrick, *Drying Milk and Milk Products*, Avi Publishing Company, Connecticut, 1971.
- 8 E. A. Diakowska, and N. S. Hall, *Solar Energy in Small-Scale Milk Collection and Processing*, Food and Agriculture Organization of The United Nations, Rome 1983.
- 9 A. R. Eswara and M. Ramakrishnarao, Solar energy in food processing—a critical appraisal, *J. Food Sci. Technol.*, 2013, **50**(2), 209–227, DOI: [10.1007/s13197-012-0739-3](#).
- 10 S. A. Kalogirou, *Solar Energy Engineering Processes and Systems*, Elsevier, London, 2023.
- 11 K. Lovegrove, W. S. Csiro, Introduction to concentrating solar power (CSP) technology, in *Concentrating Solar Power Technology*, Woodhead Publishing, Cambridge, 2012, pp. 3–15.
- 12 D. K. Patel, P. K. Brahmabhatt and H. Panchal, A review on compound parabolic solar concentrator for sustainable development, *Int. J. Ambient Energy.*, 2018, **39**(5), 533–546, DOI: [10.1080/01430750.2017.1318786](#).
- 13 O. U. Oparaku and O. C. Iloeje, Design considerations for a photovoltaic-powered water pumping facility in a rural village near Nsukka, *J. Renew. Energy.*, 1991, **10**, 64–69.
- 14 H. Schnitzer, C. Brunner and G. Gwehenberger, Minimizing greenhouse gas emissions through the application of solar thermal energy in industrial processes, *J. Cleaner Prod.*, 2007, **15**(13–14), 1271–1286, DOI: [10.1016/j.jclepro.2006.07.023](#).
- 15 J. Franco, L. Saravia, V. Javi, R. Caso and C. Fernandez, Pasteurization of goat milk using a low cost solar concentrator, *Sol. Energy*, 2008, **82**(11), 1088–1094, DOI: [10.1016/j.solener.2007.10.011](#).
- 16 M. F. Atia, M. M. Mostafa, M. F. Abdel-Salam and M. A. El-Nono, Solar energy utilization for milk pasteurization, *J. Agric. Eng. Res.*, 2011, **28**, 729–744.
- 17 G. C. Da Silva, C. Tiba and G. M. T. Calazans, Solar pasteurizer for the microbiological decontamination of water, *J. Renewable Energy*, 2016, **87**, 711–719, DOI: [10.1016/j.renene.2015.11.012](#).
- 18 M. T. A. Khan, S. M. S. Tanzil, R. Rahman, and S. M. S. Alam, *Design and Construction of an Automatic Solar Tracking System, Presented in International Conference on Electrical and Computer Engineering*, Dhaka, 2010, pp. 326–329, DOI: [10.1109/ICELCE.2010.5700694](#).
- 19 H. Panchal, R. Patel, S. Chaudhary, D. K. Patel, R. Sathiyamurthy and T. Arunkumar, Solar energy utilisation for milk pasteurisation: a comprehensive review, *Renew. Sustain. Energy Rev.*, 2018, **92**(9), 1–8, DOI: [10.1016/j.rser.2018.04.068](#).
- 20 A. Thomas and H. M. Guven, Parabolic trough concentrators—design, construction and evaluation, *Energy Convers. Manage.*, 1993, **34**(5), 401–416, DOI: [10.1016/0196-8904\(93\)90090-W](#).
- 21 L. S. Conrado, A. Rodriguez-Pulido and G. Calderón, Thermal performance of parabolic trough solar collectors, *Renew. Sustain. Energy Rev.*, 2017, **67**, 1345–1359, DOI: [10.1016/j.rser.2016.09.071](#).
- 22 A. M. de Oliveira Siqueira, P. E. N. Gomes, L. Torrezani, E. O. Lucas and G. M. da Cruz Pereira, Heat transfer analysis and modeling of a parabolic trough solar collector: an analysis, *Energy Procedia*, 2014, **57**, 401–410, DOI: [10.1016/j.egypro.2014.10.193](#).
- 23 S. Marrakchi, Z. Leemrani, H. Asselman, A. Aoukili and A. Asselman, Temperature distribution analysis of parabolic trough solar collector using CFD, *Procedia Manuf.*, 2018, **22**, 773–779, DOI: [10.1016/j.promfg.2018.03.110](#).
- 24 E. Bellos, D. Korres, C. Tzivanidis and K. A. Antonopoulos, Design, simulation and optimization of a compound parabolic collector, *Sustain. Energy Technol. Assess.*, 2016, **16**, 53–63, DOI: [10.1016/j.seta.2016.04.005](#).
- 25 S. K. Singh, M. M. Ali, C. P. Samaranayake, H. Liu, P. Setlow and S. Sastry, Effect of electric field frequency on inactivation of the *Bacillus subtilis* spore and its mutants during ohmic heating, *Food Bioprod. Process.*, 2025, **152**(7), 128–138, DOI: [10.1016/j.fbp.2025.05.006](#).
- 26 A. Bharti, and B. Paul, Design of solar parabolic trough collector, in *2017 International Conference on Advances in Mechanical, Industrial, Automation and Management Systems*, Allahabad, 2017, pp. 302–306, DOI: [10.1109/AMIAMS.2017.8069229](#).
- 27 E. Z. Moya, Parabolic-trough concentrating solar power (CSP) systems, in *Concentrating Solar Power Technology Principles, Developments and Applications*, Woodhead Publishing, Cambridge, 2012, pp. 197–239, DOI: [10.1533/9780857096173.2.197](#).



- 28 A. Duffie-John, A. Beckman-William, *Solar Engineering of Thermal Processes*, John Wiley & Sons, Inc, New Jersey, 2006.
- 29 M. Gunther and R. Shahbazfar, Solar dish technology, *Advanced CSP Teaching Materials*, 2011, vol. 1, pp. 1–63.
- 30 J. Macedo-Valencia, J. Ramírez-Ávila, R. Acosta, O. A. Jaramillo and J. O. Aguilar, Design, construction and evaluation of parabolic trough collector as demonstrative prototype, *Energy Procedia*, 2014, 57, 989–998, DOI: [10.1016/j.egypro.2014.10.082](https://doi.org/10.1016/j.egypro.2014.10.082).
- 31 A. Shirazi, R. A. Taylor, G. L. Morrison and S. D. White, Solar-powered absorption chillers: A comprehensive and critical review, *Energy Convers. Manage.*, 2018, 171, 59–81, DOI: [10.1016/j.enconman.2018.05.091](https://doi.org/10.1016/j.enconman.2018.05.091).
- 32 V. Gupta, Working and analysis of the H-bridge motor driver circuit designed for wheeled mobile robots, in *2nd International Conference on Advanced Computer Control*, Shenyang, 2010, vol. 3, pp. 441–444, DOI: [10.1109/ICACC.2010.5486818](https://doi.org/10.1109/ICACC.2010.5486818).
- 33 A. Z. Hafez, A. M. Attia, H. S. Eltwab, A. O. ElKousy, A. A. Affi, A. G. Abdelhamid, A. N. Abdelqader, S. E. K. Fateen, K. A. El-Metwally, A. Soliman and I. M. Ismail, Design analysis of solar parabolic trough thermal collectors, *Renew. Sustain. Energy Rev.*, 2018, 82(1), 1215–1260, DOI: [10.1016/j.rser.2017.09.010](https://doi.org/10.1016/j.rser.2017.09.010).
- 34 S. A. Kalogirou and S. Lloyd, Use of solar parabolic trough collectors for hot water production in Cyprus A feasibility study, *Renew. Energy*, 1992, 2(2), 117–124, DOI: [10.1016/0960-1481\(92\)90097-M](https://doi.org/10.1016/0960-1481(92)90097-M).
- 35 V. Talugeri, N. B. Pattana, V. B. Nasi, K. Shahapurkar, M. E. M. Soudagar, T. Ahamad, M. A. Kalam, K. M. Chidanandamurthy, N. M. Mubarak and R. R. Karri, Experimental investigation on a solar parabolic collector using water-based multi-walled carbon-nanotube with low volume concentrations, *Sci. Rep.*, 2023, 13(1), 7398, DOI: [10.1038/s41598-023-34529-6](https://doi.org/10.1038/s41598-023-34529-6).
- 36 C. Lamnatou, J. D. Mondol, D. Chemisana and C. Maurer, Modelling and simulation of Building-Integrated solar thermal systems: Behaviour of the system, *Renew. Sustain. Energy Rev.*, 2015, 45, 36–51, DOI: [10.1016/j.rser.2015.01.024](https://doi.org/10.1016/j.rser.2015.01.024).
- 37 P. O. Akello, C. O. Saoke, J. N. Kamau and J. O. Ndeda, Uncertainty analysis and experimental validation of solar parabolic trough collector simulation model, *Clean Energy*, 2025, zkae115, DOI: [10.1093/ce/zkae115](https://doi.org/10.1093/ce/zkae115).
- 38 P. O. Akello, C. O. Saoke, J. N. Kamau and J. O. Ndeda, Experimental validation of solar parabolic trough collector model for industrial process heat application, *Research Square*, 2024, DOI: [10.21203/rs.3.rs-3977773/v1](https://doi.org/10.21203/rs.3.rs-3977773/v1).
- 39 P. H. Dobrowsky, M. Carstens, J. De Villiers, T. E. Cloete and W. Khan, Efficiency of a closed-coupled solar pasteurization system in treating roof harvested rainwater, *Sci. Total Environ.*, 2015, 536, 206–214, DOI: [10.1016/j.scitotenv.2015.06.126](https://doi.org/10.1016/j.scitotenv.2015.06.126).
- 40 A. Solanki, Y. Pal and R. Kumar, A comprehensive review on solar assisted cooling system, *Int. J. Ambient Energy.*, 2020, 41(11), 1314–1319, DOI: [10.1080/01430750.2018.1501756](https://doi.org/10.1080/01430750.2018.1501756).

